ESKİŞEHİR TEKNİK ÜNİVERSİTESİ BİLİM VE TEKNOLOJİ DERGİSİ B- TEORİK BİLİMLER

Eskişehir Technical University Journal of Science and Technology B- Theoretical Sciences

2023, 11(1), pp. 36-42, DOI:10.20290/estubtdb.1119287

RESEARCH ARTICLE

DENSITY FUNCTIONAL THEORY INVESTIGATION ON DRUG-DRUG INTERACTIONS: ESCITALOPRAM AND SALICYLIC ACID

Musa DABOE [1], Cemal PARLAK [1] and Özgür ALVER [2]

[1] Department of Physics, Science Faculty, Ege University, Izmir, 35040, Turkey
[2] Department of Physics, Science Faculty, Eskişehir Technical University, Eskişehir, Turkey

ABSTRACT

Each year many new possible drugs have been introduced in the hope of the solution to many different medical problems or diseases. Further, many people around the world suffer from more than one health problem at a time. It is also known that some drugs are prescribed as combinations of several other drugs at once. In this study, taking the advantage of density functional theory, we have investigated the possible outcomes if someone uses escitalopram and salicylic acid at once. The obtained findings suggest that following the interaction activity of drugs is possible to change. Therefore, special care is required when using these drugs together.

Keywords: Escitalopram, Salicylic acid, Drug interactions, DFT, QTAIM

1. INTRODUCTION

In some health problems, if more than one drug has to be used together, then there is a certain possibility of drug-drug interaction (DDI) [1]. DDI, in general, is known as the effect of one drug upon another. These kinds of interactions can either produce desired or undesired results [1]. DDI might appear via chemical or physical interactions and it might occur in both pharmacodynamic and pharmacokinetic means [1-3].

Salicylic acid (SA) is a colorless organic compound with some medical applications. It is reported that SA shows antifungal, anti-infective and keratolytic characteristics [4]. It is considered as a model drug due to its extensive therapeutic use [4]. It is known as the precursor and a metabolite of widely prescribed drug acetylsalicylic acid named also as aspirin. Therefore, it is a very important molecule since aspirin appears among the most widely prescribed drugs in cardiovascular and cerebrovascular disorders for both primary and secondary prevention [5]. Along with its many useful effects, recent studies showed that aspirin is also at the cornerstone of the treatment of diabetic patients [5]. Further, it has been lately reported that low dose aspirin plays an important role in the decreasing preeclampsia and fetal diseases for both mother and the fetus [6-8]. First introduced in 2002, escitalopram (ESCI), a selective serotonin reuptake inhibitor, has been used for the condition of depression, general anxiety and panic disorder [9,10]. It is especially effective and generally well tolerated for the treatment of important generalized anxiety disorders [11].

Recently, quantum chemical calculations have been widely used for the examination of molecular structure and electronic properties of different types of molecular compounds [12]. Within these methods, density functional theory (DFT) is widely preferred and by using the concept of electron

*Corresponding Author: ozguralver@eskisehir.edu.tr
Receievd:24.05.2022 Published: 28.02.2023

density ρ, the ground state molecular and electronic properties of molecular systems can be enhanced [13, 14].

Quantum Theory of Atoms in Molecules (QTAIM) suggested by Bader has been extensively used to enlighten the covalent and non-covalent atom-atom interactions [15, 16]. In QTAIM methodology, electron density ρ, Laplacian of electron density $\nabla^2\rho$ and electronic energy density H are used to identify the nature of interaction [15]. If $\nabla^2\rho < 0$ and $H < 0$ the interaction is considered covalent or strong and if $\nabla^2\rho > 0$ and $H < 0$, the interaction is considered partially covalent and if $\nabla^2\rho > 0$ and $H > 0$ the interaction is non-covalent [17]. In the scope of this work, two widely prescribed drugs (ESCI & SA) and their interaction mechanisms were examined. Regarding the DFT calculations and QTAIM analyses, the structure and activity relationship was examined. All of the results obtained were discussed in brief.

2. COMPUTATIONAL STUDIES

Both drugs were optimized in water media without imposing any molecular limitations. Frequency calculations were also carried out as well to make sure that the obtained structures converge to a certain minimum on the potential energy surface. In any case, where the calculations produced negative frequencies, calculations were re-performed by imposing small structural changes. B3LYP functional has been extensively employed with acceptable results [18, 19]. Henceforth, calculations were performed with B3LYP functional and 6-31G(d) basis set. The binding (E_b) energies were computed as follows [20]:

$$E_b = E_{complex} - [E_{ESCI} + E_{SA}]$$

Due to its biological abundance and importance, calculations were carried out in the water phase and the polarizable continuum model was chosen to see the solvation effects [21]. Basis set superposition error (BSSE) leads to some changes in the E_b energies [22]. Therefore, possible BSSE errors were considered by using the counterpoise correction method [23]. Multiwfn, Gaussian and GaussView programs were used for the calculations and to construct the examined structures [24-26].

3. RESULTS AND DISCUSSIONS

In this part regarding the obtained data, all the drug couples were examined in groups and the important results were discussed and presented in brief.

3.1. C≡N…OH site interaction (1)

The optimized structure of the examined system was given in Figure 1. Following the interaction between the drug couples, the vibrational OH stretching band of SA shifted from 3722 cm^{-1} to 3496 cm^{-1} and the intensity of it increased from 96.9 to 2117.6. The change in the wavenumber is 226 cm^{-1} and the change in the IR intensity is around 2021 indicating that there is a serious and observable interaction at the OH edge. C≡N stretching band shifted from 2338 cm^{-1} to 2349 cm^{-1} and its IR intensity increased from 166.6 to 352.4. The change in the OH band is more apparent since the hydrogen atom is smaller than the nitrogen atom in size and it contains a smaller number of electrons and protons. Further, while there happened a 0.002 Å decrease in the bond length of C≡N causing a blue shift in the IR spectra, 0.012 Å increase was observed in the OH bond length resulting from a red-shift in the IR spectra. E_b energy for C≡N and OH site interacted system was calculated as -4.76 kcal/mol.

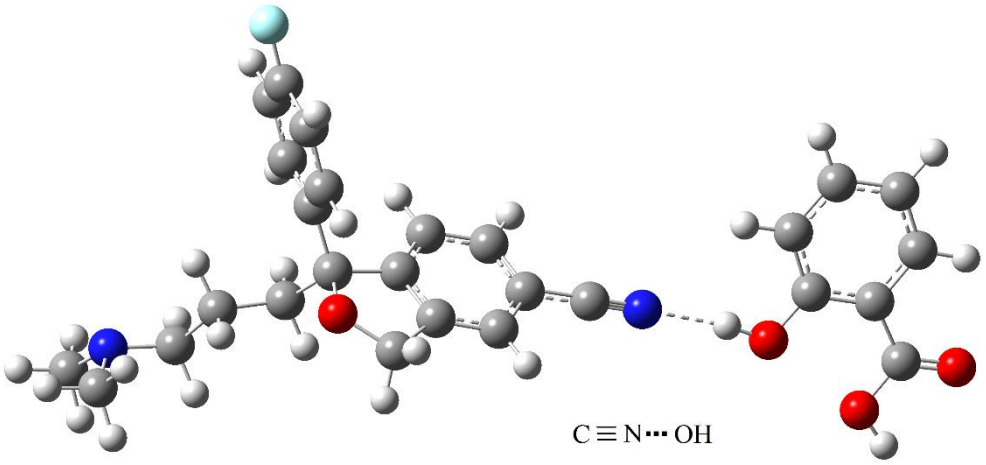

Figure 1. Optimized structure of C≡N and OH site interaction (1).

QTAIM results suggest two possible HBs occurred between C≡N…OH and C≡N…HC (ring). The first one comes with E_{HB} energy with a value of -7.58 kcal/mol and positive values of $\nabla^2\rho$ (0.0968 a.u.) and H (0.24 a.u.) which indicates a non-covalent type of interaction. Here the resultant values of H were obtained by multiplication of a factor of 10^{-4}. The second one has an E_{HB} of -0.99 kcal/mol and when compared to the first one it appears as a weak interaction. The magnitudes of HOMO-LUMO energy differences (E_g) were calculated as 5.08 eV and 4.33 eV for SA and ESCI, respectively. Following the interaction E_g reduced to 4.15 eV indicating an increase in the reactivity of the system.

3.2. C≡N…OH site interaction (2)

The optimized structure of the investigated couple was given in Figure 2. After the interaction between the drug couples, the vibrational OH stretching band of SA at the interaction site decreased from 3695 cm^{-1} to 3438 cm^{-1} and the intensity of it increased from 122.9 to 2286.2. The red-shift around 257 cm^{-1} is due to the HB interaction. C≡N stretching band altered from 2338 cm^{-1} to 2351 cm^{-1} and IR intensity of it increased from 166.6 to 317.7. At this point, it is worth to analyze the carbonyl stretching wavenumber near the interaction site. Carbonyl stretching wavenumber shifted to 1775 cm^{-1} from 1788 cm^{-1} upon interaction. Further, the IR intensity for this band decreased from 635.8 to 573.5. Following the interaction, while OH and C=O bond lengths increased by amounts of 0.012 Å and 0.003 Å, C≡N bond length decreased around 0.002 Å those agreed with trends in the change of wavenumbers. E_b energy for C≡N and OH site interacted system was found as -4.36 kcal/mol.

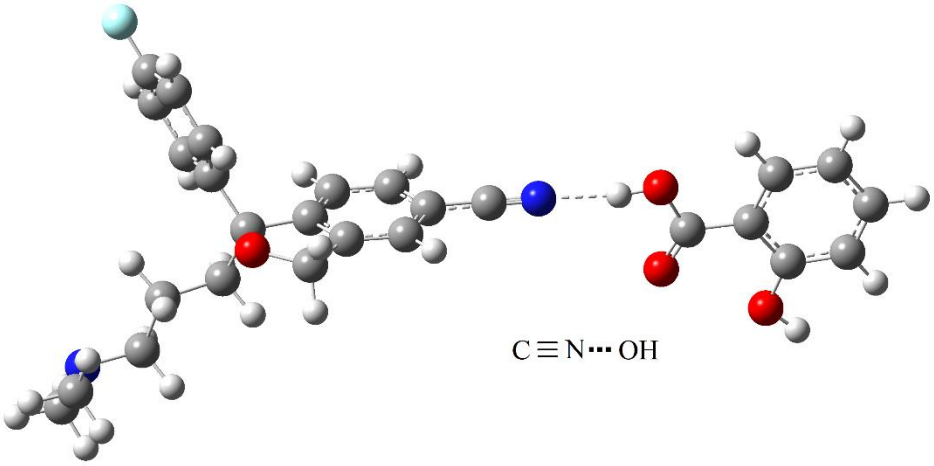

Figure 2. Optimized structure of C≡N and OH site interaction (2).

In this configuration QTAIM results suggest only one intermolecular possible HB which is between C≡N…OH with E_{HB} energy of -7.65 kcal/mol. For this interaction, while $\nabla^2\rho$ (0.0970 a.u.) was found as positive the value of H (-0.65 a.u.) was found as negative referring to a partially covalent interaction. Following the interaction E_g reduced to 4.17 eV indicating an increase in the reactivity of the system.

3.3. N and OH site interactions

The optimized structure of the investigated structure was given in Figure 3. The vibrational OH stretching band of SA at the interaction site shifted from 3722 cm^{-1} to 2855 cm^{-1} and the intensity of it increased from 96.9 to 3703.1, following the interaction. The change in the wavenumber is 867 cm^{-1} and the change in the IR intensity is around 3606 addressing a strong HB interaction at the OH edge. Following the interaction OH bond length at the interaction site increased from 0.972 Å to 1.015 Å which confirms the red-shift in the IR spectrum. E_b energy for N and OH site interacted system was calculated as -7.62 kcal/mol.

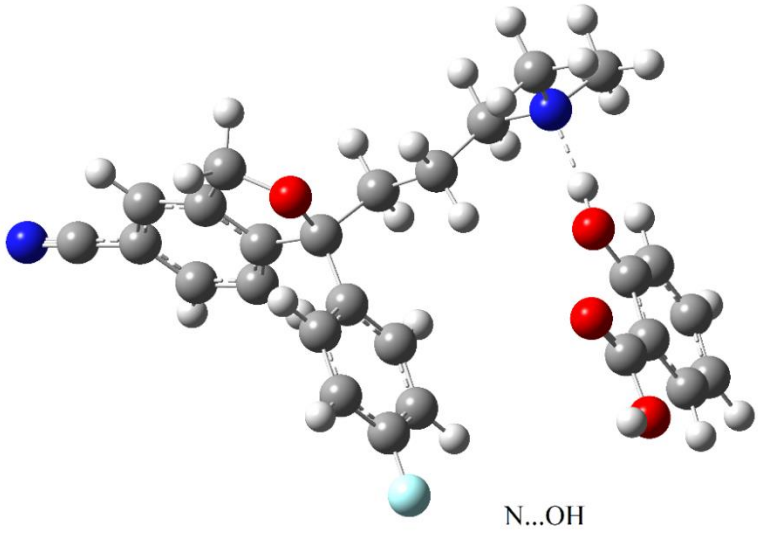

Figure 3. Optimized structure of N and OH site interaction.

In this configuration QTAIM results suggest that the strongest interaction occurs at the N…OH site with a value of E_{HB} = -12.79 kcal/mol. In this interaction, while $\nabla^2\rho$ (0.1161 a.u.) was found as positive the value of H (-58.72 a.u.) showed a negative value addressing a partially covalent interaction. E_g value of the investigated couple shifted to 4.61 eV following the interaction.

3.4. N…OH and C=O…H_3C Site Interactions

The optimized structure of the examined system was presented in Figure 4. Following the interaction, the vibrational OH stretching band of SA at the interaction site shifted from 3695 cm^{-1} to 2492 cm^{-1} and the intensity of it increased from 122.9 to 4652.5. The red-shift around 1203 cm^{-1} indicates a very strong intermolecular HB interaction. The C=O stretching vibration of SA at the interaction site shifted from 1788 cm^{-1} to 1745 cm^{-1}. The intensity of this band decreased from 635.9 to 544.8. Following the interaction, while the OH bond length at the interaction site increased from 0.976 Å to 1.037 Å, the C=O bond length shifted from 1.218 Å to 1.226 Å, respectively. E_b energy for the examined system was calculated as -7.52 kcal/mol.

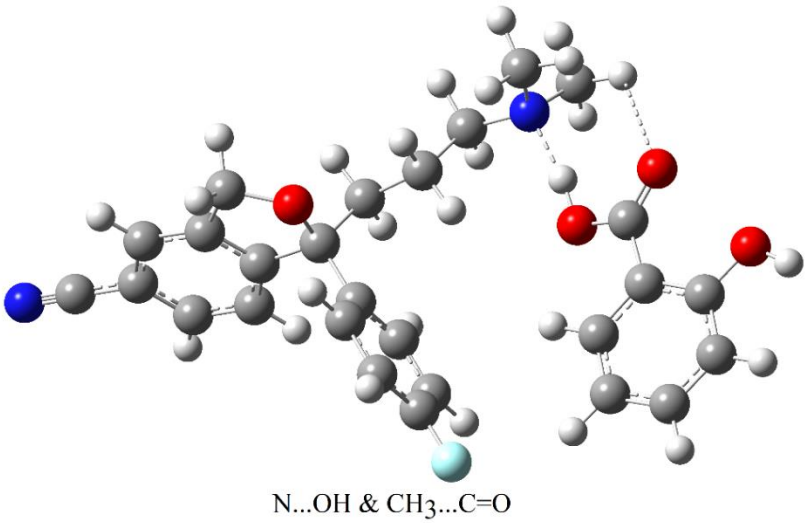

Figure 4. Optimized structure of N…OH and C=O...H_3C site interaction.

In this configuration QTAIM results propose that the strongest interaction takes place at the N…OH site with a value of E_{HB} = -16.79 kcal/mol. At this site, while $\nabla^2\rho$ (0.1284 a.u.) was found as positive the value of H (-107.18 a.u.) showed a negative value showing a partially covalent interaction. E_g value of the investigated couple shifted to 4.76 eV following the interaction.

4. CONCLUSIONS

In this study, the structure and activity relationship of ESCI and SA drug couples were investigated using DFT calculations. In summary, the following results can be summarized: The interaction between ESCI and SA drug molecules can be monitored by using infrared spectroscopy by following the changes of vibrational wavenumbers at the interaction sites. In general, the reactivity of the drug couple tends to increase compared to its components ESCI

and SA following the interaction. It was also observed that the ESCI and SA drug molecules can build inter molecular hydrogen bonds at the interaction sites. It was also seen that OH…N site interactions are stronger than OH…NC site interactions based on the E_b energy calculations.

CONFLICT OF INTEREST

The authors stated that there are no conflicts of interest regarding the publication of this article.

REFERENCES

[1] Flynn E, Drug-Drug Interactions. 2007. xPharm: The Comprehensive Pharmacology Reference, Editor: Enna SJ, Bylund DB. Boston: Elsevier. 1–3.

[2] Derry CJ, Derry S, Moore RA. Single dose oral ibuprofen plus paracetamol (acetaminophen) for acute postoperative pain. Cochrane Database Syst Revi 2013; 6: CD010210.

[3] Doherty M, Hawkey C, Goulder M, Gibb I, Hill N, Aspley S, Reader S. A randomised controlled trial of ibuprofen, paracetamol or a combination tablet of ibuprofen/paracetamol in community-derived people with knee pain. Ann Rheum Dis 2011; 70: 1534–1541.

[4] Casanova F, Santos L. Encapsulation of cosmetic active ingredients for topical application– a review. J Microencapsul 2016; 33(1): 1–17.

[5] Paseban M, Moradi Marjaneh R, Banach M, Matbou Riahi M, Bo S, Sahebkar A. Modulation of microRNAs by aspirin in cardiovascular disease. Trends Cardiovasc Med 2020; 30(5): 249–254.

[6] Cui Y, Zhu B, Zheng F. Low-dose aspirin at16≤ weeks of gestation for preventing preeclampsia and its maternal and neonatal adverse outcomes: a systematic review and meta-analysis. Exp Ther Med 2018; 15(5): 4361–4369.

[7] Roberge S, Nicolaides K, Demers S, Hyett J, Chaillet N, Bujold E. The role of aspirin dose on the prevention of preeclampsia and fetal growth restriction: systematic review and meta-analysis. Am J Obstet Gynecol 2017; 216(2): 110-120.e6.

[8] Gan J, He H, Qi H. Preventing preeclampsia and its fetal complications with low dose aspirin in East Asians and non-East Asians: a systematic review and meta-analysis. Hypertens Pregnancy 2016; 35(3): 426–435.

[9] Owens MJ, Knight DL, Nemeroff CB. Second-generation SSRIs: human monoamine transporter binding profile of escitalopram and R-fluoxetine. Biol Psychiatry 2001; 50: 345–350.

[10] Jonathan RT, Davidson MD, Bose A, Korotzer A, Zheng H. Escitalopram in the treatment of generalized anxiety disorder: double-blind, placebo controlled, flexible-dose study. Depress and Anxiety 2004; 19: 234─240.

[11] Dhillon S, Scott LJ, Plosker GL. Escitalopram A Review of its Use in the Management of Anxiety Disorder. CNS Drugs 2006; 20(9): 763─790.

[12] Dikmen G, Alver Ö, Parlak C. NMR determination of solvent dependent behavior and XRD structural properties of 4-carboxy phenylboronic acid: A DFT supported study. Chem Phys Lett 2018; 698: 114–119.

[13] Ergürhan O, Parlak C, Alver Ö, Şenyel M. Conformational and electronic properties of hydroquinone adsorption on C_{60} fullerenes: Doping atom, solvent and basis set effects. J Mol Struct 2018; 1167: 227–231.

[14] Parlak C, Alver Ö, Bağlayan Ö. Quantum mechanical simulation of Molnupiravir drug interaction with Si-doped C60 fullerene. Comput Theor Chem 2021; 1202; 113336.

[15] Bader RFW. In Atoms in Molecules: A Quantum Theory (Oxford: Clarendon Press), 1990.

[16] Grabowski SJ. What Is the Covalency of Hydrogen Bonding? Chem Rev 2011; 111: 2597─2625.

[17] Rozas I, Alkorta I, Elguero J. Behavior of Ylides Containing N, O, and C Atoms as Hydrogen Bond Acceptors. J Am Chem Soc 2000; 122: 11154─11161.

[18] Beheshtian J, Peyghan AA, Bagheri Z. Quantum chemical study of fluorinated AlN nano-cage. Appl Surf Sci 2012; 259: 631–636.

[19] Peyghan AA, Soltani A, Pahlevani AA, Kanani Y, Khajeh S. A first-principles study of the adsorption behavior of CO on Al-and Ga-doped single-walled BN nanotubes. Appl Surf Sci 2013; 270: 25–32.

[20] Hazrati MK, Hadipour NL. Adsorption behavior of 5-fluorouracil on pristine, B-, Si-, and Al-doped C60 fullerenes: A first-principles study. Phys Lett A 2016; 380: 937–941.

[21] Tomasi J, Mennucci B, Cammi R. Quantum Mechanical Continuum Solvation Models. Chem Rev 2005; 105: 2999–3094.

[22] Boys SF, Bernardi FD. The calculation of small molecular interactions by the differences of separate total energies. Some procedures with reduced errors, Mol Phys 1970; 19: 553–566.

[23] Simon S, Duran M, Dannenberg J. How does basis set superposition error change the potential surfaces for hydrogen-bonded dimers? J. Chem. Phys. 1996; 105: 11024–11031.

[24] Lu T, Chen F. Multiwfn: A multifunctional wavefunction analyser. Journal of Computational Chemistry 2012; 33: 580–592.

[25] Frisch MJ, Trucks GW, Schlegel HB et al. Gaussian 16, Revision C.01, Gaussian Inc., Wallingford, CT. 2016.

[26] Dennington RD, Keith TA, Millam JM. GaussView 6.0.16, Gaussian Inc., 2016.